MMTO Technical Memorandum #03-8

Smithsonian Institution &
The University of Arizona®

In Situ Aluminization of the MMT 6.5m Primary Mirror

W. Kindred, J.T. Williams, D. Clark

June 2003

In Situ Aluminization of the MMT 6.5 m Primary Mirror

W. Kindred, J. T. Williams, and D. Clark
MMT Observatory, 933 N. Cherry Ave., Rm. 460, Tucson, AZ 85721
bkindred@mmto.org, jtwms@as.arizona.edu, dclark@mmto.org
http://www.mmto.org/MMTpapers/pdfs/tm/tm03-8.pdf

MMTO Technical Report **#03-8**, June 2003

Abstract

On May 20, 2000 the MMT Conversion was dedicated. Space limitations on the summit of Mt. Hopkins, AZ and limited financial resources dictated in situ aluminization of the ϕ6.5 m primary mirror. Some of the attendant challenges successfully addressed in the course of accomplishing that task are described. For example: a 22 metric ton, ϕ7 m vacuum head had to be lifted 25 m before being lowered through the horizon-pointing telescope truss (clearing by 16 mm), then secured to the mirror cell that serves as a vacuum baseplate; dirty mirror-support hardware integral to the cell required isolation of the process volume operating at 10^{-6} mbar; extensive modeling of source geometry was needed to achieve uniformity goals at very short source-substrate distances; limited facility power capacity led to development of a self-contained, battery-powered PWM circuit that allowed simultaneous firing of 200 evaporation sources. Details of design and construction of the evaporation system are given along with techniques and results of the successful coating in November 2001.

I. Introduction

From May 1979 to March 1998, before its conversion to a single ϕ6.5 m aperture, the MMT on Mt. Hopkins (south of Tucson, AZ) operated as a multiple telescope platform. An alt/az mount in a rotating building provided a footprint small enough to allow the MMT to be located atop the near-conical 2,606 m summit. The images from its six ϕ1.8 m Cassegrain telescopes were superposed to give the equivalent light gathering area of a single ϕ4.5 m telescope. Since four reflections were required for this superposition, production and maintenance of the highest quality reflecting films were a priority from the outset. Over a twenty year period, deposition processes were refined to the point that strongly adhering and highly reflective (reflectance equaling that of films condensed under ideal conditions[1-7] as well as calculated values[1]) aluminum (Al) films could be consistently produced.

The six co-mounted telescopes have now been replaced by a single classical Cassegrain of ϕ6.5 m aperture with an f/1.25, monolithic, honeycombed, borosilicate primary mirror. Thin film objectives for the conversion remained ambitious, and included a structure function error budget[8-10] corresponding to an atmosphere of $r_0 = 400$ cm or 5 nm rms surface error.

Because of limited space available for facilities on Mt. Hopkins (Figure 1), unconventional approaches to observatory development had to be considered. In addition to the substantial expense, a separate deposition facility would have created a number of difficult issues. The mechanical and

Figure 1. The MMT atop Mt. Hopkins near Tucson. Photo courtesy of S. Criswell (FLWO).

storage facility (at the top, or east, in Figure 1), for example, would likely have been forced offsite—a very problematic option. The daunting complexity and risk of removal, transportation, and reinstallation of the primary mirror made in situ aluminization appear to be the only viable alternative. The cost and other benefits of in situ coating had been well outlined,[11-13] and budget limitations may have dictated such an approach even if space weren't an issue. A glance at Figure 2, which shows the primary mirror dangling above the telescope, should convey the trepidation felt here at the thought of doing it any other way!

Economy and uniformity requirements (which, with a short source-substrate distance, implied a substantial number of sources) largely drove the process of deciding just how to put Al on the mirror. The first attempt incorporated several ambitious time and money saving innovations involving the use of series-connected, ϕ2.5 mm tungsten (W) rods to thermally evaporate Al in vacuo. While showing promise in some respects, these efforts ultimately failed and are not discussed here—suffice to say that in the coating business things are done the way they are for a reason, usually one borne of hard experience. (That adventure might be the topic of a future discourse.) Next, a more conventional approach utilizing parallel W filaments was adopted, several more modern and energetic techniques being rejected as too expensive and/or difficult to implement on a large scale.

Figure 2. The ϕ6.5 m mirror is lowered into its cell March 25, 1999. Photo courtesy of Marco Crane.

Several years of dedicated team (and individual) efforts culminated November 9, 2001 with the first successful in situ aluminizing of a ϕ6.5 m-class mirror. Even with a sizeable perforation in the partitioning membrane, which increased pressure in the process volume an order of magnitude above target, reflectance was better than 91% at 450 nm and adhesion was good.

II. Coating Objectives

MMTO facility instruments cover the spectral range of 320 nm to 10 μ, making unprotected Al the only reflecting material suitable for the primary mirror. Protective oxide overcoats[2,7,14-22] usually have absorption bands in the thermal infrared that can dramatically increase emissivity, exhibit significant losses at high angles of incidence, show transmission dips near 3 μ due to water adsorption, and impose significantly increased complexity and cost on the deposition system.

Reflectance, scattering, adhesion, and durability of evaporated Al films are a function of several interdependent deposition parameters listed below in order of importance:

- Deposition rate[3]—the higher the better (however, see exception below). It is well established that the properties of thin Al films are more dependent on deposition rate than any other single parameter. Al is very reactive: ultraviolet (UV) reflectance begins to decay within seconds at a total pressure of 7×10^{-6} mbar due to the formation of an oxide layer.[23] Low deposition rates promote incorporation of greater quantities of oxides and other contaminants[24] in the film: granularity, scattering, and total hemispherical emittance[25] increase while reflectance and density decrease. Al films deposited at low rates show greater deterioration in UV reflectance with age.[2] Blue (400 nm) reflectance of Al deposited at 4×10^{-6} mbar begins to roll off as deposition rates fall below 2 nm/sec—this is the minimum acceptable rate;

While there should be no upper limit on deposition rate, reflectance of films produced in smaller systems used by the observatory (with much shorter source-substrate distances, 30-45 cm) begins to roll off as rates exceed about 10 nm/sec. This is likely due to substrate heating as reflectance measurements are usually made on witness plates of 1 mm thickness. Other possibilities exist, however, including nucleation and other atomic collisional processes in the vapor cloud, as well as increased production—and consequent incorporation—of volatile W oxides.[26] Further, as evaporation rate increases so does the likelihood of "spits" and "comets"[27] that, if deposited on the substrate, will eventually become sizeable pinholes and deterioration foci. Ten nm/sec is the maximum acceptable rate;

- Pressure[3]—the lower the better. Al is an efficient getter and oxidizes readily; mean free path (mfp) should be substantially in excess of source-substrate distance. Decreasing pressure reduces dependence of reflectance on deposition rate[1] and retards effects of aging on UV reflectance. Evaporation at higher pressures,[28-30] even in a non-oxidizing atmosphere, is viewed here with suspicion. While reflectance of films produced in argon (Ar) and hydrogen (H_2) atmospheres of 10^{-4} mbar (mfp $\approx$ 0.6 m) appears to be near ideal,[29,30] no work on the morphology of such films has surfaced. The available literature consistently suggests that collisional energy loss with resultant decrease in adatom surface mobility and packing density at these pressures could have significant implications for scattering and durability. Holland[26] also notes that the level of heater material incorporated in a film rises linearly with pressure for a fixed evaporation rate, although this effect is probably small. Target system ultimate pressure is 1.3×10^{-6} mbar (mfp $\approx$ 50 m);

- Evaporant incidence angle[31]—specular reflectance decreases quantitatively near vapor incidence angles of 30° and is down as much as a few percent at 60°.[1] This is principally a consequence of angular growth of the columnar microstructures that effectively increases grain size and scattering.[32] Density of films so structured is less than normal, the increased porosity providing more surface area for the adsorption of water and other contaminants. Source baffles are designed to limit vapor incidence angle to 60° in the worst case;

- Film thickness (t)[1]—opacity and reflectance approach maximum at a thickness of about 60 nm (λ=650 nm).[33] Rms roughness of Al films increases approximately as $t^{1/2}$ while total integrated scatter increases as t^2.[34] Losses in specular reflectance and increases in scattering are discernible, depending on conditions, by about t=200 nm. As thickness increases so does sensitivity to the effects of increasing vapor incidence angle, increasing pressure, and decreasing deposition rate. Tensile stresses accumulate with thickness, increasing the likelihood of cracking, flaking, pinholing, and delamination.[35] Since no difference is observed here in the durability of just-opaque and thick Al films, everything points to the desirability of going thinner rather than thicker. Target thickness is 95 nm;

- Evaporant purity[2]—99.5% Al produces measurably inferior results. Very nearly ideal reflectance can be obtained with evaporant purity of 99.99%. "Five-nine" (99.999%) Al is readily available, inexpensive, and used here;

- Glow discharge cleaning[36,37]—fresh films at MMTO have always been required to pass a "Scotch® tape" adhesion test. The principal determinant of adhesion is inclusion of proper glow discharge cleaning immediately prior to evaporation—without it, the most stringent final cleaning process and perfect "black breath"[38] will give passable results an unpredictable percentage of the time. Ion bombardment also accelerates desorption of water vapor and other contaminants from chamber surfaces, which can then be removed. Oxygen (O_2) is required for efficacious removal of hydrocarbons and production of strongly adhering Al films. Ideally the substrate is uniformly immersed near the positive column side of the cathode dark space, particle velocities being near maximum there. While cleaning is perhaps most efficient in this region, it takes place sufficiently throughout the volume for acceptable results;

- Pinhole population[27,39-42]—durability and scattering are a function of pinhole density. Most pinholes result from particle contamination of the surface. While every vacuum deposition chamber is a particle factory, guaranteeing pinholes in even the most meticulously prepared films, considerable reduction can be made in the initial population by thorough carbon dioxide (CO_2) "snow" cleaning[42-48] prior to closing the chamber, and roughing the chamber slowly to minimize turbulence;[49]

- Substrate temperature (t)[1,7]—Al (and other low melting point metals such as silver, gold) deposited on heated substrates ($t > 100\,°C$) agglomerates into grainy, high-scatter films. This presents no problem as the primary mirror must be kept near ambient temperature; it will not safely withstand appreciable temperature gradients. Negligible substrate heating occurs during deposition.[50]

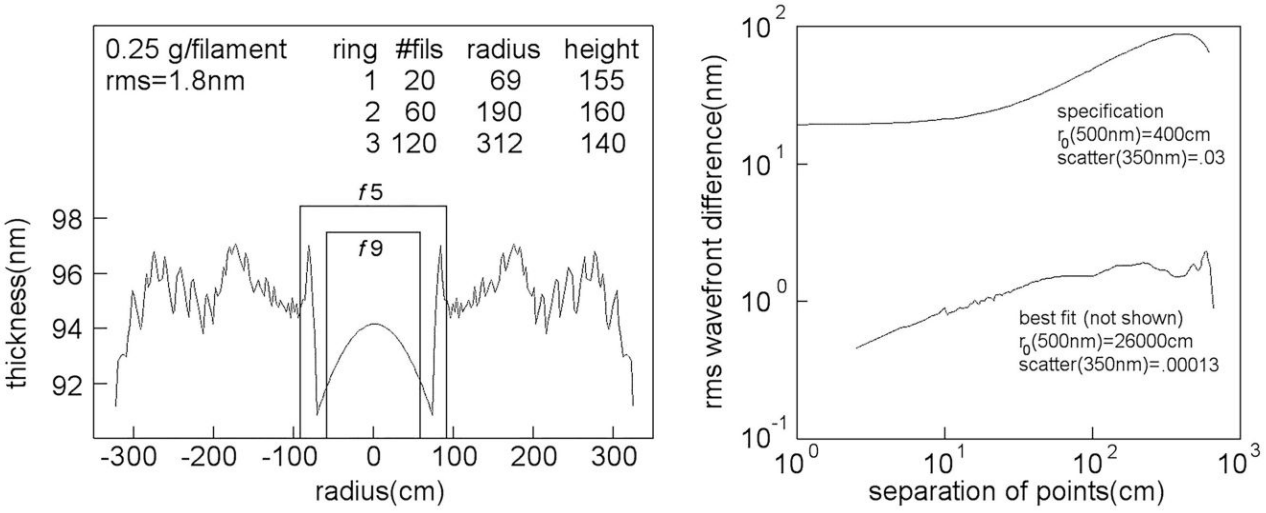

Figure 3. Model thickness profile (left) and structure function.

III. Source Geometry

The structure function error budget for the primary coating corresponds to 5 nm rms surface irregularity. The source-substrate distance is physically constrained to approximately 1.5 m—a distributed array is consequently required to meet uniformity requirements. A system of concentric rings provides a simple, effective solution. Software authored by J. M. Hill (LBT) was used to model thickness distribution vs. array geometry. Inputs were number of rings, ring radii, ring heights above the parabolic vertex, number of evenly spaced point sources per ring, and cone baffle angle. Numerous iterations produced an optimal solution having 200 sources on three concentric rings at varying heights (all near 1.5 m) above the mirror. A diametral cut of thickness distribution and structure function are shown in Figure 3; the solution is graphically depicted in Figure 4.

The high spatial frequency, steeply sloped structure in the model output (using point sources) is mitigated by the three-dimensional extent of the real sources. As discussed later, the structure is additionally smoothed by concentric ring baffles, which are used instead of circular cans over each source. The rms error is reduced further by eliminating the central regions occulted by $f/5$ and $f/9$ secondary shrouds. While the distribution is not yet empirically verified, nothing in the star-illuminated telescope pupil gives cause to doubt that it conforms reasonably well to the model. Finally, note that a predicted quarter gram of Al per source is evaporated uniformly into 4π sr to condense 95 nm on the mirror surface.

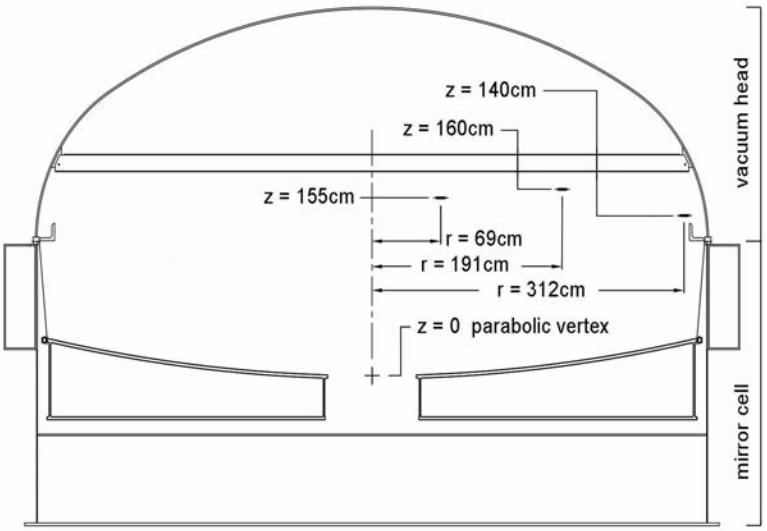

Figure 4. Filament ring geometry.

IV. Vacuum Head

Figure 5 shows a cutaway view of the ϕ6.8 m vacuum head assembly. One of the ϕ1.3 m cryopumps can be seen along with its isolation valve, one ϕ0.8 m central port, and a stand weldment. Also seen is the source ring support structure, or "star" (of David). It is constructed of 6061-T6 Al I-beams, from which are suspended the source rings. Empty weight (including the star) is 14,100 kg. Two cryopumps and gate valves add approximately 6,800 kg. Stainless steel is the material of choice for vacuum vessel fabrication, but the MMT vacuum head is constructed of mild steel to reduce cost. Inner surfaces of the vessel are painted with AKZO Cat-A-Lac 463-3-100 low vapor pressure epoxy. The cured epoxy outgasses at a rate of about 10^{-8} mbar-l/sec/cm^2,[51,52] comparable to clean, outgassed mild steel, and about an order of magnitude better than slightly oxidized mild steel.[53] The vacuum head/mirror cell combination was helium (He) leak checked before applying the epoxy and exterior paint.

While the vacuum properties of the epoxy appeared to be suitable, there were still reservations, the collective experience being limited to stainless steel and glass. How would the epoxy react to ion and evaporant bombardment, to irradiation and primary electrons from glow electrodes? Would it fracture with diurnal and seasonal thermal cycling (the head is stored outside on the summit) and expose the mild steel? No quantitative evaluation of these concerns is offered, but after living on the summit for four years and undergoing six vacuum cycles and four source firings as of this writing, the epoxy is performing beautifully. It is also nearly impervious to solvents and mild acid/base solutions, making cleanup and maintenance straightforward. The 463-3-100 formulation is no longer produced, but paints with similar qualities are presently available, e.g., Aeroglaze A276 from Lord Corporation (see Appendix A).

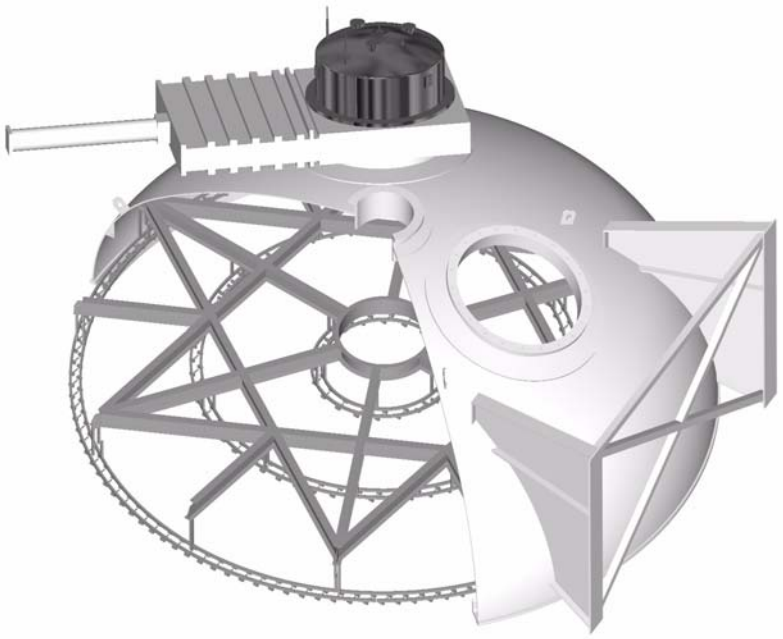

Figure 5. Cutaway rendering of partial vacuum head assembly.

IV.a. Source Rings

Source rings are rolled from 1" 6063-T5 Al square stock. This alloy is inexpensive, readily available, has low quantities of volatile constituents, good weldability, and very low resistivity—just 80% higher than that of OFHC copper (Cu). Cu is not used because of its weight, cost, and affinity for corrosion. Any competent metal shop should be able to roll the squares to the correct radius without introducing significant warpage. Figure 6 shows the innermost ring assembly including shields and support columns. The smaller-radius, continuous ring serves as electrical common while the outer is split into 5-filament segments. The ½" x 1" rectangular tabs are welded to the major segments and provide a means for keeping the filaments horizontal—the vacuum head axis of symmetry is horizontal in operation. With vertical filaments, gravity will, at some point, overcome surface tension. Sizeable Al charges (1 g) cannot be reliably held on typical filaments at arbitrary orientations with respect to gravity. (The actual required load turns out to be much smaller, however, and might work at any orientation—see page 15.)

Shuttering capability for the sources was discussed and the idea dropped as too complex (and, more importantly, time consuming) for the current iteration. This might be revisited at some point—shuttering has several benefits—although it now seems unlikely as their presence is demonstrated to be not required for acceptable results.

Al square drops are used for the columns that attach the rings to the support structure. Electrical isolation is accomplished with polycarbonate (Lexan®) washers and sleeves. Outgassing properties of polycarbonate are surprisingly good at room temperature[52] although care must be taken to isolate it from heat sources.

IV.b. Filaments

Filaments are made to the following specifications:

- 6” overall length
- 3” wrap length
- 3 x ϕ.03” W wire
- 12 x ϕ.5” i.d. coils

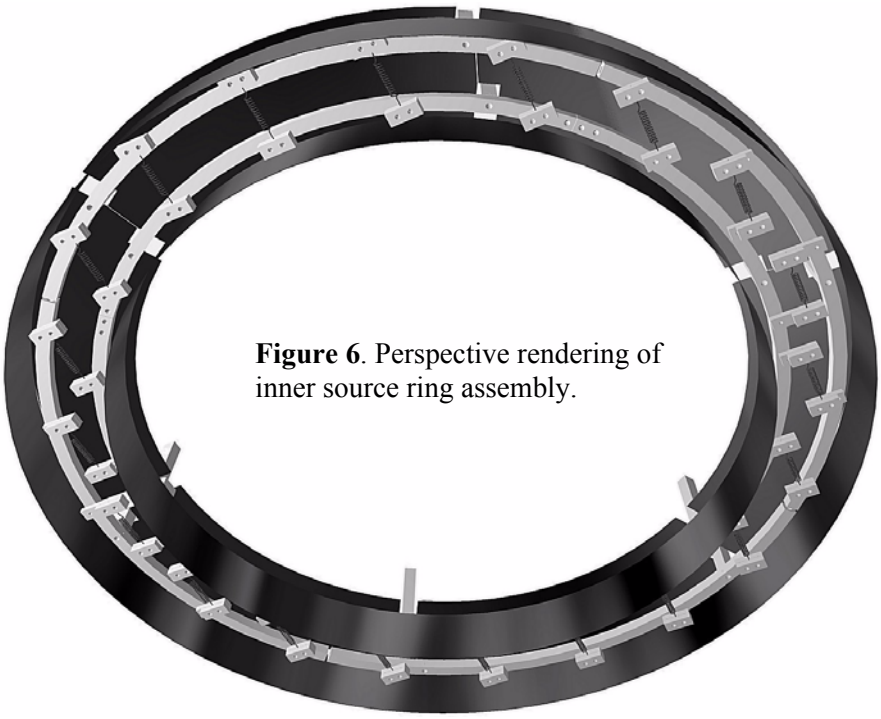

Figure 6. Perspective rendering of inner source ring assembly.

Experiments determined that these filaments could hold one evenly-distributed gram of Al without pooling if properly loaded and wetted. Figure 7 illustrates the loading method. The filament coils are wrapped with 425 mm of ϕ1.0 mm Al wire (0.90 g), 4-5 tightly wound turns per coil, spanning coil-to-coil. The spans are then cut—with no shorted coils, heating is very uniform and predictable. This method also puts each coil load in good mechanical and thermal contact with the W, further encouraging consistent behavior. The Al is wrapped on the side of the coils toward gravity (after installation) to prevent pooling upon melt. The software model prediction of 0.25 g Al evaporated per source notwithstanding, filaments were charged, for this first shot, with 0.9 g of evaporant material—it was intended that they not run dry under any circumstance. Filaments are resistance matched and weighed individually before and after loading to ensure electrical and load uniformity. The wrapped filaments are then etched in an ultrasonic bath of phosphoric and nitric acid immediately prior to installation. This is an important step: even though oxides form slowly on W, they do form and Al will not wet them. Also, W contamination in Al films produced with unetched filaments has been observed.[7] As a precaution against losing any power modules during the shot, filament banks (there are 40 individual banks of five filaments) are interleaved throughout the vacuum head so any single-point power failure would impact more or less uniformly on the mirror surface.

Test-fired filaments remain supple enough after one firing to tempt repeated use, but it has been decided to use new filaments each shot for the following reasons:

- uniformly reloading partially spent sources would be problematic and labor intensive. It is nearly impossible to reload in place without physically disturbing the embrittled filaments, and the environment in which this work would have to be done is hardly conducive to precision and detail;
- in the smaller systems a quantitative decrease in reflectance per shot on a given filament has been consistently observed—cause unknown;
- even if partially spent sources could be reliably recharged, the startup current requirements of pre-wetted filaments might be prohibitive for the power supply;
- cost of filaments ($1.2k) is small when viewed as a percentage of the overall expense of realuminizing.

IV.c. Source Shielding

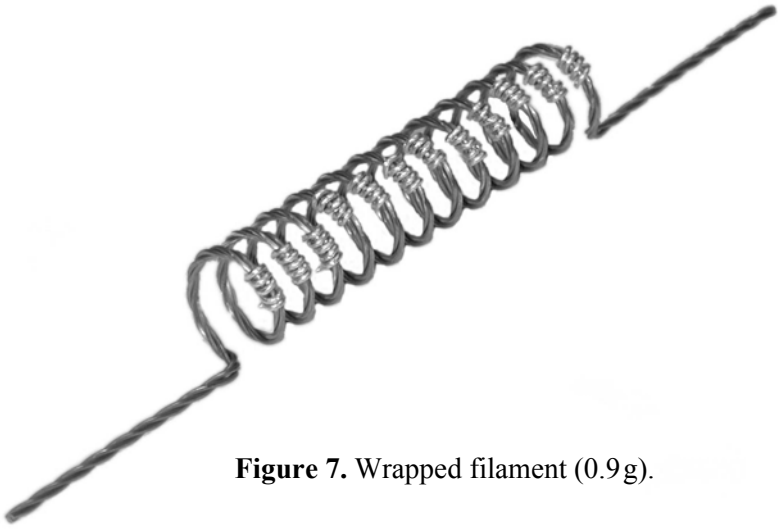

Figure 7. Wrapped filament (0.9 g).

In an ideal system, evaporated Al atoms would impinge only on the mirror surface, condensation on other surfaces producing mainly deleterious effects. A system of stainless steel sheet metal walls and annuli arranged in a basic π configuration (Figures 6 and 8) contains the bulk of evaporant not directed at the mirror. These baffles also serve the principal function of limiting vapor incidence angle. The concentric inner and outer walls are located in r and z so as to limit the evaporant incidence angle at any point on the mirror surface to about 60°. The original plan had cylindrical cans over each source, but this was abandoned in mid-construction as too labor intensive and time consuming. A simple CAD ray trace confirmed the efficacy of this revised arrangement, although its impact on film distribution, while probably small, is unknown and needs to be modeled. These baffles have to be accessible or removable as they will need periodic cleaning. They also serve the function of preventing glow electrode primary electrons from reaching the substrate or cryopump. The concentric wall arrangement additionally mitigates the slopes and high spatial frequency structure in the deposited film.

V. Vacuum System

The volume at 10^{-6} mbar is 80,000 l with a geometric surface area of 150 m^2. The original design called for this volume to be evacuated by three ϕ1.3 m cryopumps, although there was some disagreement about the need for that much speed and capacity. Much of the initial testing took place with only one valved cryopump, and on the basis of those results it was decided that two cryopumps would be sufficient. The mirror cell volume is roughly equivalent to the front volume with a great deal more surface area. Roughing is accomplished with an 850 m^3/hr rotary vane pump backing a 10,000 m^3/hr Roots blower. Appendix B is a schematic diagram of the system.

V.a. Roughing System

Figure 9 illustrates the layout of the roughing system. The mechanical pump and blower are permanently secured to a flatbed trailer, which makes for easy transport and offsite storage. Roughing lines are ϕ12" schedule 80 PVC irrigation pipe coupled with neoprene sleeves. A gap is forced between adjoining sections of pipe. As the lines are evacuated, barometric pressure (750 mbar) draws the sleeves into contact with smooth, filleted surfaces for the pressure seal. This scheme is very inexpensive and provides flexible seals that are He leak-tight to 10^{-8} mbar-l/s. PVC initially outgasses at about 1.3×10^{-6} mbar-l/s/cm^2,[52,53] roughly the same as dry fluoroelastomer (Viton®). Outgassing by the roughing line material represents less than 1% of the gas load at 10^{-2} mbar.

The line comes into the telescope chamber through the rear exterior wall before bifurcating to the mirror cell and vacuum head. At each end of the bifurcation is a liquid nitrogen (LN_2)-cooled, optically dense chevron baffle and ϕ30 cm right-angle, pneumatic poppet

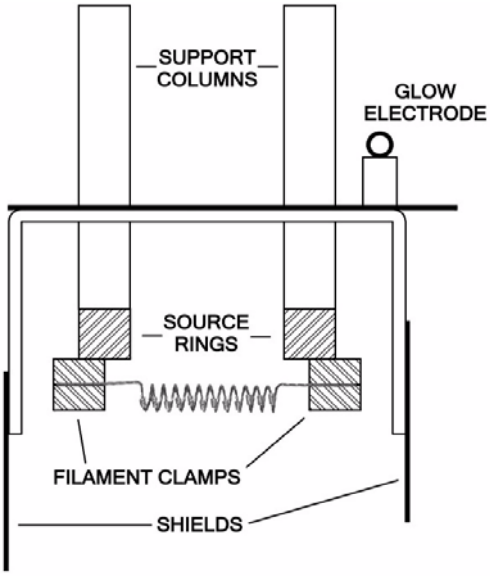

Figure 8. Source ring assembly in cross section.

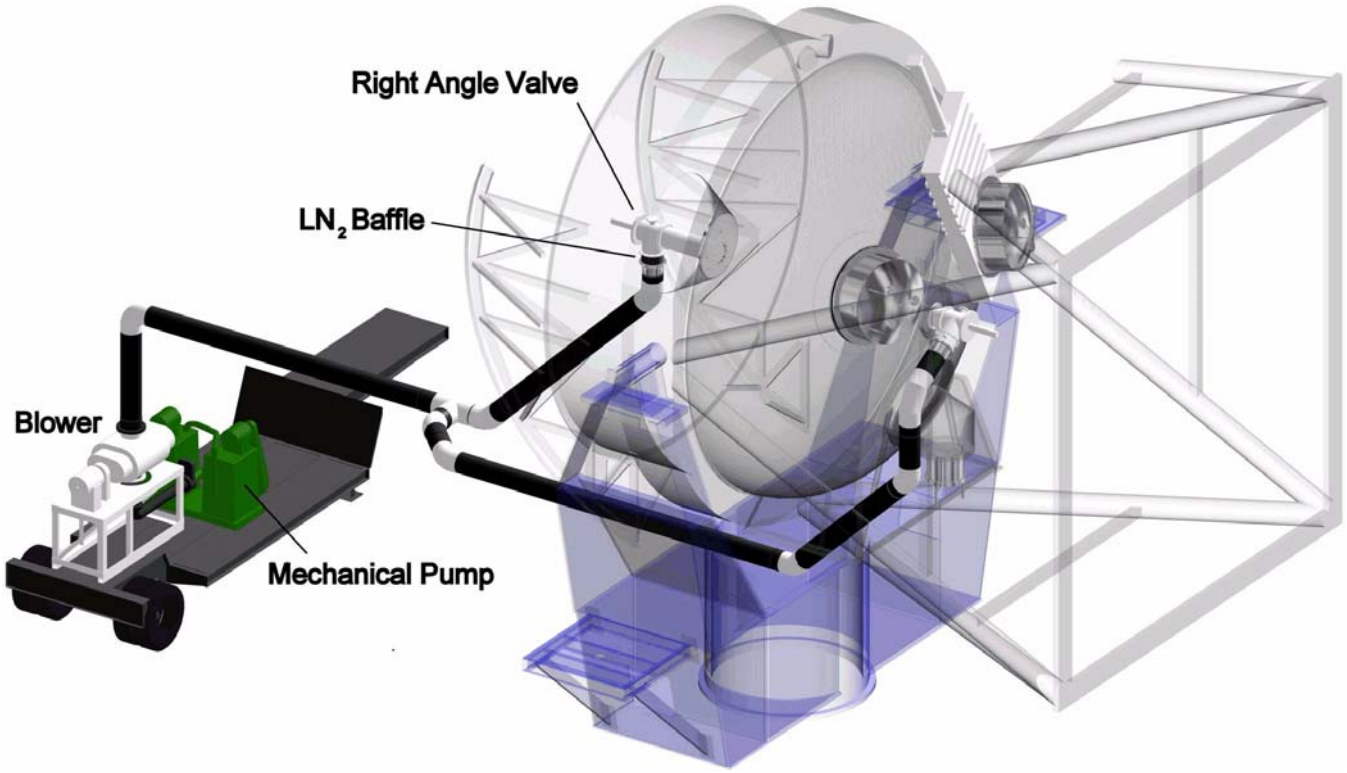

Figure 9. Roughing system.

valve. The cold traps are necessary to prevent backstreaming from the roughing pumps during transition, and greatly enhance the roughing system's ability to remove water vapor. The ϕ30 cm valves are bypassed by ϕ5 cm valves that, with feedback from a 0±10 mmHg differential capacitance manometer, allow adequately precise pressure control during the initial stages of pumpdown—pressures in both vacuum regions can't be allowed to differ by more than a few mbar without risking rupture of the pressure membrane. In viscous flow, line conductance losses are about 20%. In all pressure regimes, conductance is limited by the chevron baffle, and one could effectively argue that the rear baffle is unnecessary, the mirror cell being such a dirty environment that worrying about backstreaming seems unnecessary (see, however, the discussion of reflectance on page page 15). Even with the baffle installed, the mirror cell can easily be held at 3×10^{-2} mbar, which for an estimated effective pumping speed of 2000 ℓ/s, implies a total gas load in the mirror cell of about 50 mbar-ℓ/s.

V.b. High-Vacuum System

The decision to use cryopumps for evacuation to working pressure was made early in the design process. The staff had no experience with capture pumps, and some paranoia crept in as rumors concerning performance and reliability surfaced early in the familiarization period. A conservative philosophy was adopted: preserve, to the extent practicable, cryopumps for process only—finding other means of accommodating chamber conditioning, glow discharge cleaning, etc.—and cross over at the lowest pressure obtainable. The main component of this solution is a 6,000 ℓ/s turbomolecular pump. It can be started toward the low end of the blower range (10^{-2} mbar) and will pump the chamber to about 10^{-5} mbar. The turbo is backed through a ϕ5 cm pickoff from the roughing line.

Two closed-loop, gaseous helium cryopumps with throat diameters of ϕ1.32 m are used. The first stage is LN_2-cooled with a reservoir capacity of a few hours. Three 12 W cold heads refrigerate the second stage (charcoal) to 11 K. At the MMT's request, the cryopump manufacturer increased the charcoal area about 50% to provide greater thermal inertia as well as higher light-gas pumping speed. This should enhance the system's ability to cope with the expected H_2 surge prior to evaporation (the origins of which are not completely understood although H_2

evolution resulting from dissociative adsorption of water molecules[24,54] is known to occur in abundance throughout the evaporation). H_2 pumping speed was measured at the manufacturing facility in excess of 110,000 l/s at 1.3×10^{-6} mbar. No crossover recommendation was provided but similar pumps from other manufacturers list crossover capacities of about 900 Torr-l. For this capacity and a volume of 8×10^4 l, crossover pressure is 1.5×10^{-2} mbar. The unpleasant prospect of roughing to pressures this far into the transitional range drove the decision to include the LN_2 baffles in the roughing lines, and reinforced the argument for the turbopump. (At the point these decisions were made, the possibility of having cryopumps without valves was very real—with valves, they can be pumped down offline. The front baffle is still needed to rough the process volume to the turbomolecular pump start pressure (≈0.05 mbar) as it does not, and will not, have an isolation valve.)

It is now believed, in hindsight, that the gas capacities of the cryopumps amply allow for crossover at more reasonable pressures (0.25 mbar) where backstreaming is not a consideration. According to the manufacturer's numbers (Ar capacity = 6,000 atm-l, similar for nitrogen) crossover at 0.25 mbar could be accomplished hundreds of times before approaching capacity. The turbopump is still a very desirable tool—while the process could succeed without it, comfort and safety margins are certainly larger with it. Being able to hold the chamber while regenerating a cryopump and having an absolute backup in case the cryopumps become saturated or overwhelmed by the gas load is a decided advantage, as is being able to condition the chamber independent of the cryopumps.

In a cryopumped system it is necessary to shield the first-stage (80 K) chevron from any source of heat or fast electrons. To accomplish this there are throat-diameter stainless discs located one radius from the effective cryopump apertures. Conductance is minimally impacted while the bulk of radiation incident on the chevron is intercepted.

As part of the original scheme, Meissner traps and other means of external cryocondensation pumping to augment the cryopumps were discussed—again, the principal concern being management of the H_2 surge (i.e., water vapor). At the time it wasn't very clear whether H_2 production resulted primarily from dissociation of free or adsorbed water vapor. Evidence suggesting the latter surfaced,[30] so further removal of free water vapor appeared to be of comparatively little value, certainly vis-à-vis the trouble and expense. Cryocondensation coils would also be of no value in pumping light gasses such as H_2. The best thing that could happen regarding management of water vapor would be to aluminize during a dry part of the year instead of in the heart of monsoons—the MMT closes for maintenance and recoating during the annual period of daily rain, mid-July through early September. As will be seen later, however, the water problem turns out to be much less intractable than was originally suspected.

V.c. Pressure Membrane

The body of the honeycombed, borosilicate mirror must be isodynamically pressurized; the stresses induced by an atmosphere pushing on one side would be unacceptably high. This means the entire mirror has to be under vacuum with the backside exposed to a very unclean environment. The gas load imposed by the mirror cell would make pumping the entire volume to 10^{-6} mbar prohibitively expensive, if not impossible. Some means of isolating the front surface of the mirror from the cell is required. Polyester (Mylar®) film aluminized on one side is used as a barrier material with the coated side toward lower pressure. The outgassing rate of very thin polyester aluminized on both sides is higher by an order of magnitude after about 30 minutes.[55] The dominant material outgassed in the short term is absorbed water, which outdiffuses rapidly toward the uncoated side. The MMT has no data on permeability of these membranes, but empirical results suggest gas load from any source associated with them is negligible. Figure 10 illustrates the membrane system in cross section.

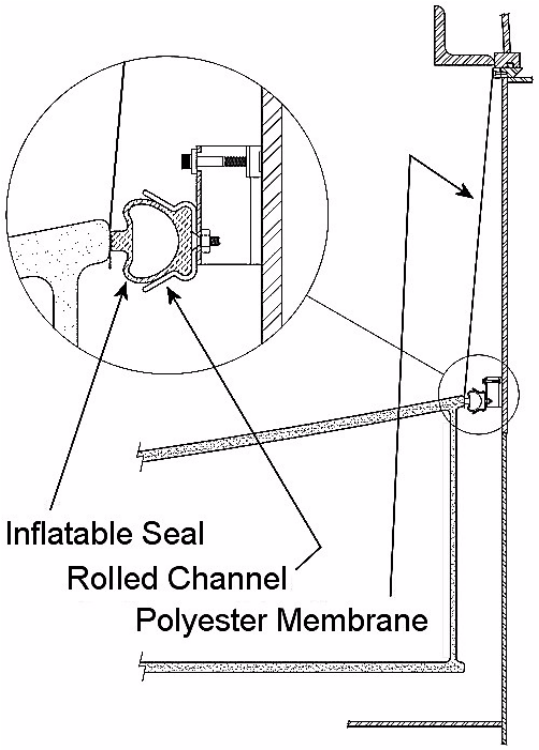

Figure 10. Pressure membrane.

The membrane is clamped at the top of the mirror cell so as to encompass the elevation axle covers and the cell perimeter wall, which are anything but clean after years of atmospheric exposure. The membrane surface area is 17.5 m^2—a 1 mbar pressure differential applies a force of about 400 lbs. With 1 atm in the inflatable seal, burst pressure is somewhat in excess of 15 mbar (determined the hard way) with a 0.05 mm membrane. This figure could be highly variable. While it should never be needed in this capacity (in fact, it already has), the membrane doubles nicely as an absolute pressure relief system (burst disc) protecting the mirror from significant pressure gradients. If the membrane ruptures, time to recover to the same point is about two days.

Membranes of 0.05 mm and 0.006 mm thickness have been used. The thicker material presumably tolerates greater pressure differentials and has lower permeability. It definitely presents problems with pleating in one or both seal locations. An improved design would have the membrane represent the wall of a cylinder rather than that of a cone frustrum, reducing or eliminating the pleating problem. Pleats appear to be no impediment for the thinner material, and the degree of isolation obtainable is the same for both.

The process of evacuation starts with 1 atm (gauge) in the inflatable seal. In order to limit radial forces exerted on the primary mirror frontplate, this pressure must be reduced proportionally as pressure in the vacuum head drops so that as the latter approaches zero, the former approaches 1 atm (absolute)—see schedule in Appendix C.

For this shot the Cassegrain perforation was covered with the same polyester film. An Al, o-ring sealed center plug with a remotely activated ϕ0.36 m butterfly valve will be implemented in the future. With this valve open, the pressure differential during roughing should be more easily managed, and worry-free roughing of both volumes through the mirror cell might be possible. The plug will double as a cleaning seal and funnel (with the butterfly valve assembly removed). A fluoropolymer resin (Teflon®) coating should protect the Al plug from cleaning chemicals while contributing minimally to the process gas load (this is to be determined).

VI. Glow Apparatus

Glow electrodes are rings of ϕ16 mm 3003-H14 Al tubing (rolled rod would have been a better choice from a vacuum standpoint). This alloy is almost 99% Al, much less expensive and more readily available than 1100. Two continuous electrodes are located just above the top shield on the middle and outer source ring assemblies at radii 200 and 319 cm, heights 172 and 152 cm. A power supply rated at 5,000 VAC and 500 mA drives the electrodes, one of which is a floating ground. A stable, uniform glow discharge at 10 μ requires about 700 V at 400 mA. Series W-filament light bulbs on the input side of the power supply regulate current and suppress surges.

VII. Power System

The power system needs to be compact and portable. A bank of truck-starting batteries can provide high-enough power density and not tax the 150 k*W* generator that supplies backup power for the observatory complex of eight major telescopes (the coating operation is normally carried out on generator because the local power grid is unreliable during monsoon thunderstorms). A completely charged bank of forty 12 V batteries would deliver the required current for the necessary duration. The principal design task is to develop a reliable control system for smoothly and uniformly applying power to the filaments. Management of the multiple DC circuits is accomplished through a pulse-width modulation (PWM) control topology.

This system works on the principle of rapidly switching a DC source to produce a desired rms power level. Ten power modules, all having a common return (neutral bar), are used to drive 200 filaments. The modules are paired in five power units that function as bipolar supplies, each polarity driving 20 filaments. Thus, each module pair cancels the output current, maintaining a net of zero current in the neutral bar. The neutral bar arrangement creates an important system constraint: all modules have to be closely synchronized to completely cancel the return current. A substantial imbalance could push more current through the return conductor than it could safely handle.

The PWM system depends on a single master clock (800 Hz) that begins the switching cycle. Once enabled by the operator, the clock turns all power modules on and applies current to the filaments. Differential amplifiers sense the voltage at the vacuum head feedthroughs, and this signal is integrated during the PWM on-time. The integrator output ramp is then compared to a setpoint voltage selected by the operator. The PWM signal is forced off as the level exceeds the setpoint, and the cycle repeats at the next master clock pulse. The master clock duty cycle and the integrator slope at maximum circuit output are designed to produce a guaranteed off-period in every PWM cycle to maintain system controllability. Circuit impedances are very well matched because of care taken in the preparation of individual filaments and the high conductance of the filament connections. This keeps the PWM turn-off points, while slightly different for each circuit, phased well enough to prevent sizeable imbalances. The clock can be shut down and all power modules turned off at any time by the operator via a locking toggle switch.

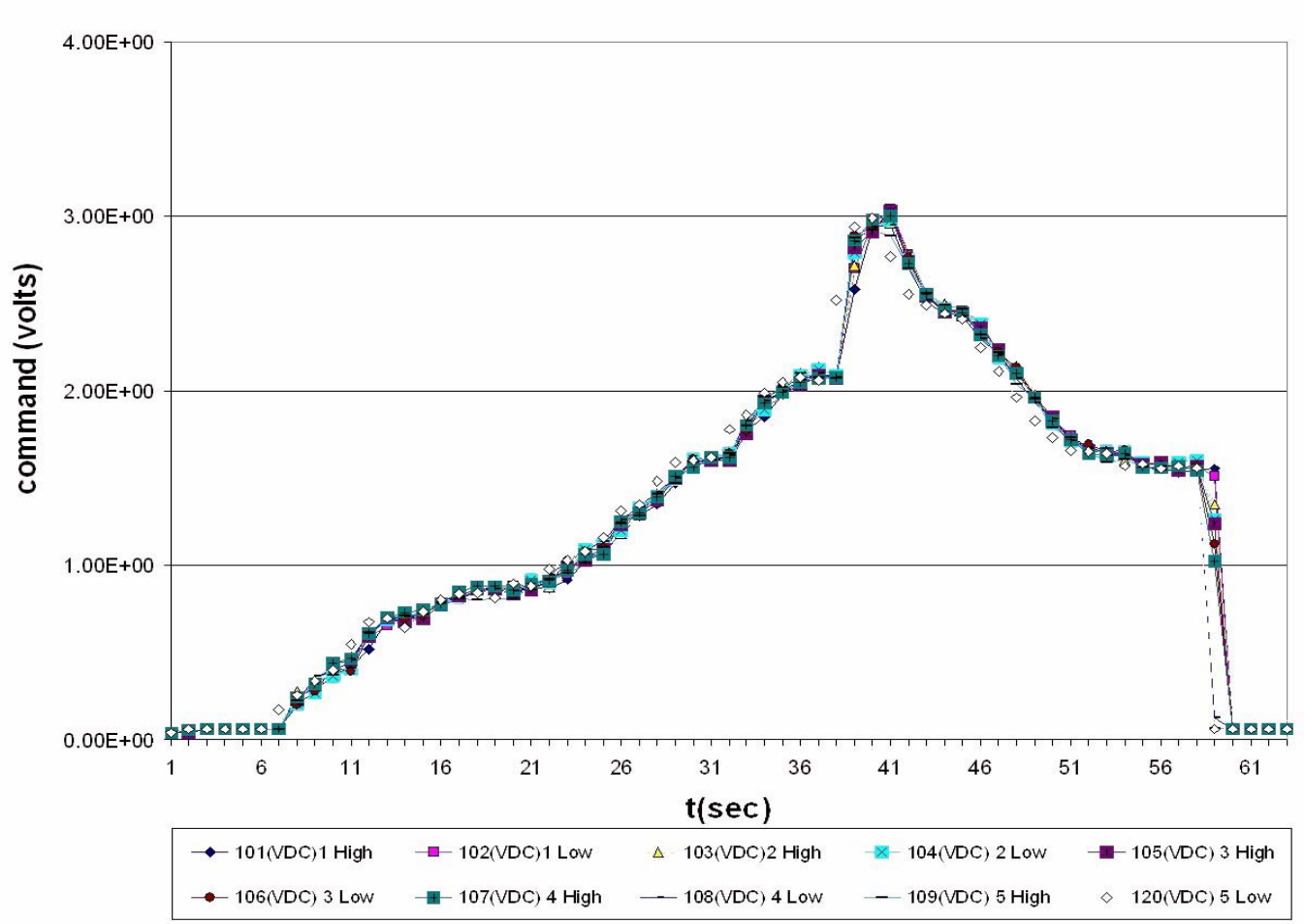

Figure 11. Power module tracking 11/9/01.

Each power module is connected to 24 VDC from four 12 V, series-parallel batteries. The modules consist of MOSFET switching elements, a driver card for the MOSFETs, and a snubber circuit to protect the switching elements from spikes. The combination of cable, connection, and load impedances results in 1100 A peak switching currents when the (unwetted) filaments are at ambient temperature. These large switching currents necessitate great care in design, assembly, and testing of the modules—cleanliness of the bus bar plates and connection bolts is critical, as is proper assembly technique. Any contamination by metallic chips in the bus "sandwich" over the MOSFETs leads to a short; module failure will rapidly ensue because of the snubber circuit's inability to prevent localized overvoltages. It is important to check the entire circuit with a megohmmeter before installing the MOSFETs.

To minimize power losses in the modules, parallel MOSFETs with the lowest possible on-resistance are used; most circuit losses result from cable and internal battery resistance. The design calls for MOSFETs with an ultimate V_{ds} rating of 60 VDC. Stray inductance in the MOSFET circuit, coupled with the rapidly switching currents, produces

a high “kickback” voltage when the PWM signal is turned off. This very destructive spike is quenched by a snubber circuit of surprisingly non-trivial design. The mechanical arrangement of the power modules, snubbers, and gate-drive circuits is optimized to minimize stray inductance and maintain switching reliability—a power module failure during process would produce large imbalance currents and possibly require discontinuing the shoot.

Component cooling is a major issue—low on-resistance notwithstanding, a large amount of power is dissipated across the MOSFETs. The switches are thermally common to massive, finned heat sinks—not massive enough, as it turns out. Forced air cooling proved inadequate. The heat sink fins needed to be submerged in water before the modules could operate at maximum output for a complete cycle without exceeding the MOSFET’s temperature limits.

For real-time monitoring, each module has an instrumentation output that provides the operator with a total power indication. This output is driven by a peak-detection circuit on the integrator outputs of the feedback system, scaled to provide the appropriate voltage level for the front-panel displays at 100% output. The same signal is scaled to 5V for the data acquisition system.

The complete system is contained in three 3’ x 4’ x 5’ roll-around steel cages. Current lines to the vacuum head are braided and stranded double-ought Cu. The electromagnetic fields around the wires are strong enough to require careful shielding of sensitive electronics.

On November 9, the system described here successfully synchronized and drove all filament banks to within a few percent during the deposition (Figure 11). There are some safety concerns still being debated regarding the switching of high currents around highly charged batteries—modern, compact welding inverters are being investigated as the basis for an alternate scheme. Appendix D is a schematic diagram of the power system.

VIII. Mirror Preparation

The mirror is stripped and cleaned while zenith pointing, the forward face of the mirror cell trunnion providing a stable work platform (Figure 12). Four-mil thick polyethylene sheet replaces the polyester for this step. The runoff is funneled through the central perforation and collected in 275 gal. high-density polyethylene containers where it is pH neutralized before disposal. Water (10 MΩ min.) is supplied through a three-bed deionization system. Chemicals are applied with untreated cotton mop heads on extension handles. These mop heads have been washed twice in a very dilute industrial detergent solution and thoroughly rinsed before use. Our stripping procedure[56] is outlined as follows:

- Clean water rinse to soften contaminants and dislodge particulates;
- Light scrub (mopping) with industrial detergent (e.g., Liquinox®, Alconox®) solution and rinse;
- Repeat as necessary (usually twice);
- Thorough rinse, change mop heads;
- Light scrub with Al stripper (dilute HCl and Cu_2SO_4 solution) and rinse;
- Repeat as necessary (usually twice);
- Thorough rinse, change mop heads;
- Light scrub with $CaCO_3$ and dilute KOH solution, rinse;
- Repeat as necessary (usually three times);
- Thorough rinse, change mop heads;
- Light scrub with dilute HNO_3;

- Long rinse and quick towel dry;
- Final surface cleaning with reagent grade isopropanol, wiped dry. This step is a bit of a trick, requiring several workers in clean-room suits, gloves, and booties to be on the mirror surface (Figure 13). The anhydrous solvent is applied and feverishly wiped dry before having an opportunity to evaporate. Used towels are flung over the side after a few swipes and workers on the trunnion face are continuously supplying fresh towels to the radial line of cleaners working their way backwards around the mirror. This technique produces adequate, if not perfect, results—very few residual cleaning artifacts have been visible in the finished product.

Figure 12. The old aluminum is removed.

Few precautions are taken during this cleaning process regarding particulate contamination. In over twenty years of preparing mirrors for aluminization at the Sunnyside facility, no substrate has ever been damaged. At Sunnyside, mirrors are stripped and cleaned outside, in open air during desert monsoon season with its attendant atmospherics. Perhaps some luck is involved but proper technique renders the process largely insensitive to any effects from airborne particulates.

Figure 13. The surface receives a final wipe with very pure isopropanol.

After stripping, the pressure membrane is installed and a protective plastic sheet secured over the mirror. The telescope is then lowered to near-horizon pointing and secured. The upper "Vee" section of the truss is removed to allow insertion of the vacuum head, and rails upon which the vacuum head will rest are placed inside the chamber. The head is then lifted from its storage position atop the facilities building and set face-down on the parking lot. In a separate operation it is tilted to vertical (Figure 14), then lifted and lowered into the telescope structure (Figure 15). A week of preparatory work ensues: roughing line assembly, removal of primary actuators and hardpoints, installation of vacuum covers on the mirror cell, final electrical checks, potting of creases in the membrane with low vapor-pressure resin, preparation and placement of witness samples, final inspection and CO_2 cleaning of the mirror, securing the vacuum head to the mirror cell, instrumentation checkouts—to name just a few.

IX. Aluminization 11/01

On November 9, 2001 the system described here was used to aluminize the primary mirror. Initial pumpdown was delicate owing to the membrane's pressure intolerance. While the pumpdown procedure could easily be automated in the future, biofeedback closed the loop for this shot. Each bypass valve was manned and differential pressure continuously monitored. The bellows valves in place at the time were not well suited for the task and required frequent adjustment. This roughing method necessarily kept the pressure time constant well below that at which turbulent redeposition of significant numbers of particulates was likely.[49] The Roots blower was started at 50 mbar. Two hours into the process, chamber pressure was below 3 mbar. At this point the large roughing valves were opened and turbine spin-up started. Three hours later the chamber pressure had dropped to 2×10^{-5} mbar.

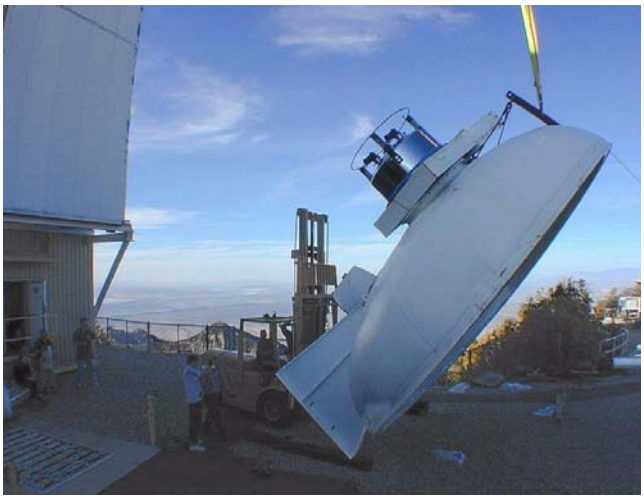

Figure 14. The vacuum head is tilted to vertical.

Ar and O_2 were admitted to a pressure of 1.5×10^{-2} mbar and a glow discharge was sustained for 30 minutes. O_2 was quenched and the glow continued for 15 minutes. Here, the usual procedure was modified because a valve for the second cryopump did not yet exist. This required bringing the pump to an operational state after the glow discharge cleaning, and introduced a four hour delay from end of glow to beginning of evaporation. Such an interval negated some—perhaps most—effects of glow discharge cleaning, but it did not render the glow valueless. With both cryopumps evacuating the chamber, pressure again stabilized at 2×10^{-5} mbar—much higher than expected. No He leaks were found on the chamber side, but one of the mirror cell cover seals had collapsed, producing a sizeable leak. He was detected at this fault by a mass spectrometer located in the process chamber—the pressure membrane was also perforated. Since the cell was holding at 25×10^{-3} mbar and the chamber at 2×10^{-5} mbar, it was decided to shoot. The higher cell pressure was of no consequence and it was known from experience that Al films of acceptable quality could be condensed at that process pressure.

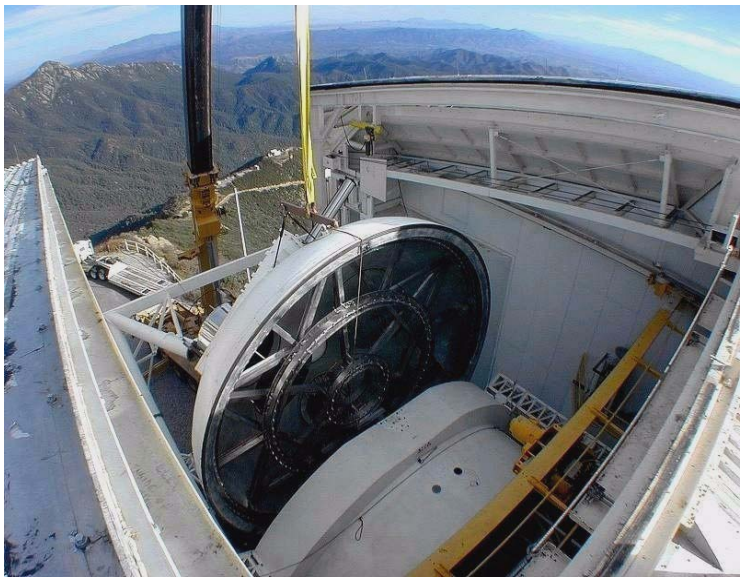

Figure 15. The vacuum head is lifted over the telescope structure (left) and lowered into place (right).

The evaporation phase of the process went perfectly. A quartz crystal microbalance at the innermost mirror zone (r = 50 cm) recorded 93 nm of Al deposited in about 20 seconds. A second monitor at the mirror outer edge (r = 320 cm) measured 102 nm. The difference, if real, would be in reasonable conformance with model predictions. More precise characterization of the system can take place when hardware for offline operation becomes available (2005). The peak deposition rate topped 7 nm/sec, at which point the power system was at 60% duty cycle. Unfortunately, the data collection system, or more precisely, the author who had only catnapped during the previous 72 hours, malfunctioned—much of the detailed data in handy form were lost but backup monitoring salvaged the essentials. Chamber pressure and deposition rate vs. time are presented in Figure 16. Note that the much-feared H_2 surge was easily handled by the cryopumps (charted pressure values are uncorrected—the H_2 peak at 30 seconds should be expanded X2 above the air background).

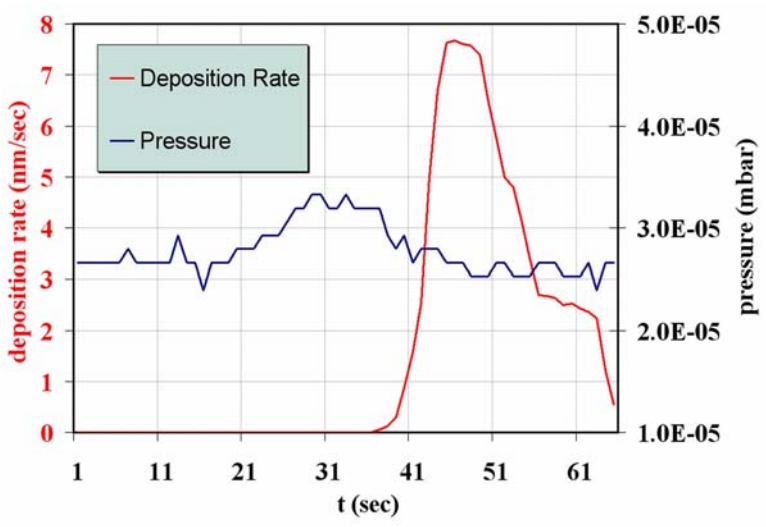

Figure 16. Pressure and deposition rate vs. time.

Reflectance of an edge witness plate is charted in Figure 17. While 91% is very acceptable, it is not as high as it should be—the smaller systems produce Al films that reflect more than 92% at 450 nm. Neither the high deposition pressure nor lack of an effective glow immediately before evaporation should account for such a reflectance loss. It might be significant that the gas load was heavily contaminated (coming through the mirror cell). In hindsight, it would have been wise to cool the rear baffle once evidence of a membrane perforation presented itself. Recently uncovered issues with reflectance measuring equipment also could account for the discrepancy. Much more will certainly be learned next shot, currently scheduled for August 2004.

All filaments were of uniform appearance and had much of the 0.90 g Al charge remaining. Nine filaments from uniformly distributed locations were removed and weighed: mean weight = 17.26 g, σ 0.087 g. The new, unloaded filaments averaged 16.54 g, σ 0.003 g. Therefore, the amount of evaporated Al per filament is about 0.2 g, in general agreement with the model prediction. The 0.90 g loads were as conservative as had been hoped and will be reduced in the future by half or more. There was no appreciable sagging or physical distortion of the sources. The weight deviation and remarkably similar appearance of all the filaments attested to a very uniform burn.

All witness samples and several locations on the inner and outermost zones of the primary were tape-tested within an hour of opening the chamber—no Al was lifted.

An opening in the pressure membrane that appeared to have an area of several cm^2 was discovered at the perforation for the edge thickness monitor head. Several smaller perforations were also found around the perimeter seal. This is consistent with observations—assuming an effective pumping speed of 100,000 ℓ/s (air) and no other gas load, the ultimate pressure of 2×10^{-5} mbar gives the leak a throughput of 2 mbar-ℓ/s: at the mirror cell pressure of 25×10^{-3} mbar, this would correspond to an area of 7 cm^2.

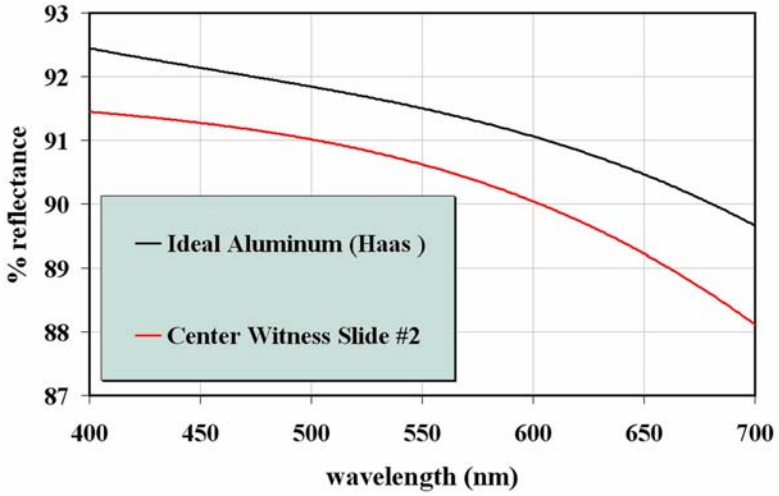

Figure 17. Spectral reflectance measured with Minolta CM-2002 Spectrophotometer.

X. Conclusions

It has been demonstrated that, while certainly not trivial, the complications of in situ aluminization for a 6.5 m class mirror are manageable. In answer to the challenges posed, the MMT observatory has developed the following:

- an easy, practical method of storage and transport for roughing-system pumps
- inexpensive, portable, vacuum plumbing for remotely located pumps
- a system for storage, maneuvering, and balancing a 20 ton vacuum head
- methodology for transforming a mirror cell into a vacuum chamber
- a workable scheme for partitioning vacuum regions and successfully maintaining good evaporation pressure on one side
- a method by which both volumes can be evacuated while maintaining a differential pressure of no more than a few mbar
- a power system that can simultaneously fire hundreds of filaments without consuming site capabilities
- a method for producing highly uniform coatings with source arrays very close to the substrate

While the converted MMT has yet to experience a fault-free aluminizing cycle, it is shown that practicable solutions to the above issues are within reach.

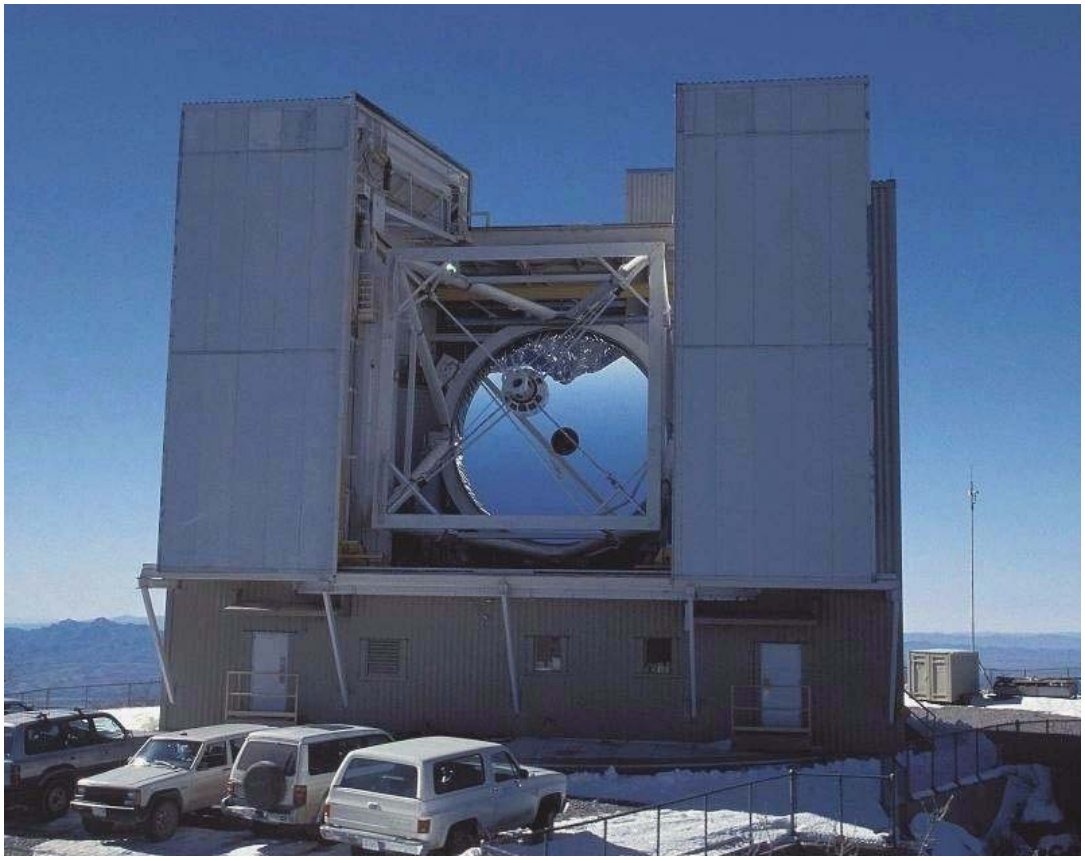

The converted MMT ready for high-throughput science, 11/12/2001.

XI. Acknowledgements

This work represents the collaborative effort of people too numerous to individually acknowledge but the authors would like to thank for their particularly significant contributions Carol Heller, John McAfee, Alejandra Milone, Ricardo Ortiz, Michael Alegria, Cory Knop, and Brian Comisso of MMTO, and Michael Orr of Steward Observatory—they made the ideas come to life. Also appreciated is the helpful feedback of Dr. John Hill (LBT), Dr. Gary Schmidt (MMTO), and assistance with preparation of the manuscript by Barbara Russ (MMTO).

APPENDICES

Appendix A. List of Suppliers

Agilent Technologies
(*data acquisition unit*)
395 Page Mill Rd.
P.O. Box 10395
Palo Alto, CA 94303
(800)452-4844
http://we.home.agilent.com

Associated Vacuum Technology, Inc.
(refurbished vacuum equipment)
832 N. Grande Ave.
Covina, CA 91724
(626)967-3869
http://www.avtvac.com

GNB Corp.
(gate valves)
3200 Dwight Road
Suite 100
Elk Grove, CA 95758
(916)395-3003
http://www.gnbvalves.com

International Rectifier
(*high-speed, high power MOSFETs*)
Thom Luke Sales
9700 North 91st St., Suite A-200
Scottsdale, AZ 85258
Tel:(480)451-5400
http://www.irf.com

Lord Corporation
(*vacuum paints*)
Chemical Products Division
(Lord Coatings Technologies)
1625 Riverforks Drive
East Huntington, IN 46750
(800)458-0434
http://www.lord.com/markets/aerospace.htm

Maxtek, Inc.
(*crystal monitors*)
11980 Telegraph Rd.
Ste. 104
Santa Fe Springs, CA 90670
(562)906-1515
http://www.maxtekinc.com

Metallized Engineering (MEI)
(*aluminized polyester*)
120 Bowles Rd.
Agawam, MA 01001
(413)786-6300
http://www.metallizedengineering.com

Minolta Instrument Systems Division
(*spectroreflectometer*)
101 Williams Drive
Ramsey, NJ 07446
(201)529-6060
http://www.minoltausa.com

MKS Instruments
(*pressure instrumentation*)
6 Shattuck Road,
Andover, MA 01810-2449
(800)227-8766
http://www.mksinst.com

Oxford Instruments (Austin Scientific)
(*cryopumps*)
4114 Todd Lane
Austin, TX 78744
(512)441-6893
http://www.oxinst.com

Presray Corp.
(*inflatable seals*)
159 Charles Colman Blvd.
Pawling, NY 12564-1193
(845) 855-1220
http://www.presray.com

Space Environment Laboratories, Inc.
(*low vapor pressure resins*)
P.O. Box 1061
Boulder, CO 80306
(303)443-4090

Sycon Instruments
(*crystal monitors*)
6757 Kinne St.
E. Syracuse, NY 13057
(315)463-5297
http://www.sycon.com

Varian Vacuum Technologies
(*turbomolecular pump*)
121 Hartwell Ave.
Lexington, MA 02421
(800)882-7426
http://www.varianinc.com

Appendix B. Vacuum system schematic

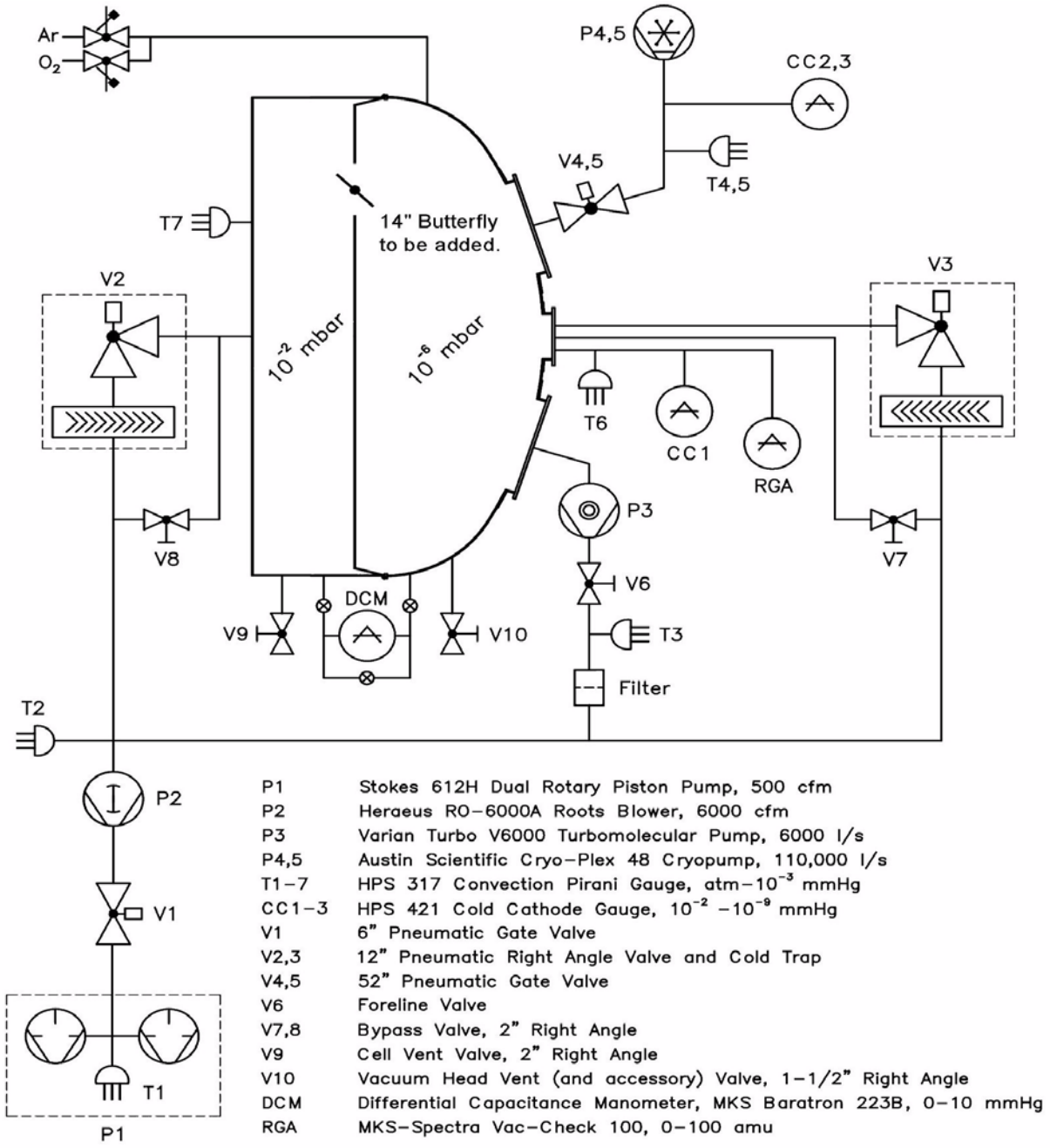

P1	Stokes 612H Dual Rotary Piston Pump, 500 cfm
P2	Heraeus RO-6000A Roots Blower, 6000 cfm
P3	Varian Turbo V6000 Turbomolecular Pump, 6000 l/s
P4,5	Austin Scientific Cryo-Plex 48 Cryopump, 110,000 l/s
T1-7	HPS 317 Convection Pirani Gauge, atm-10^{-3} mmHg
CC1-3	HPS 421 Cold Cathode Gauge, 10^{-2} -10^{-9} mmHg
V1	6" Pneumatic Gate Valve
V2,3	12" Pneumatic Right Angle Valve and Cold Trap
V4,5	52" Pneumatic Gate Valve
V6	Foreline Valve
V7,8	Bypass Valve, 2" Right Angle
V9	Cell Vent Valve, 2" Right Angle
V10	Vacuum Head Vent (and accessory) Valve, 1-1/2" Right Angle
DCM	Differential Capacitance Manometer, MKS Baratron 223B, 0-10 mmHg
RGA	MKS-Spectra Vac-Check 100, 0-100 amu

MMT Conversion Coating Facility
System Schematic

Appendix C. Aluminizing SOP

6.5m Aluminization Standard Operating Procedure

B. Kindred, J.T. Williams

Version of April 8, 2003

I. Initial Conditions

- Summit on generator power
- Pressure membrane, center plug in place and sealed
- Thickness monitors tested—crystal life and oscillation frequency recorded, witness samples cleaned and in place
- Final inspection of mirror surface and any necessary touchups complete. Mirror surface CO_2 cleaned
- Rear covers secured to mirror cell. Torque and seal clearance verified
- Onboard flange inspected, cleaned and, if necessary, repaired
- Belljar closed, temperature and relative humidity recorded
- Operation of all valves tested
- Pumps, roughing lines plumbed to belljar and cell
- Power supply system connected to filament array and tested for open and short circuits. There should be $\geq 200\Omega$ between signal and earth ground—$\approx 1.5\,m\Omega$ from any feedthrough to return
- 2000 liters LN_2 delivered to summit
- Cryopumps fully operational: regenerated, rate-of-rise pressure tested, compressors connected, He charged and preconditioned, coolant circulating
- Batteries fully charged
- Pressure transducers calibrated
- Pressure instrumentation connected and verified
- Ar and O_2 (glow gas) lines to belljar purged
- Data acquisition system (HP34970A) checked—power and pressure parameter feeds connected and tested
- DCM (differential capacitance manometer, 0 ± 10 Torr) manifold valves open. Equalization valve closed
- V9 & V10 (cell and belljar vent valves) closed

II. Roughing

1. Verify building air is ON—should indicate ≈ 120 psi. *If roughing line evacuation begins without air pressure holding V2 and V3 (12" right angle valves) closed, the pressure membrane(s) will rupture.*
2. Open V7 (front bypass valve) 3 turns, V8 (rear bypass valve) 4 turns.
3. Open V4, 5 (52" gate valve).

4. Start P1 (mechanical pump, aka Stokes). Open valve V1 (6" gate).
5. Adjust V7 and V8 as necessary to maintain equal pressure in the belljar and cell (0 indicated on DCM, max. ±1.0).
6. Pressure in the inflatable perimeter seal must be reduced with belljar pressure. Never exceed 13 psi absolute—this could possibly overstress the mirror frontplate.

   Reduce seal pressure according to the following schedule:

Chamber Pressure (mmHg)	Seal Pressure (psi gage)
560	10.8
280	5.4
140	2.7
70	1.4

7. Start P2 (Roots blower or blower) at 25 Torr.
8. Open V2 and V3 (cell and belljar 12" right angle valves) at or below 1Torr.
9. Cool front baffle.

   Notes: º At some point the operator should visually monitor inflation/deflation of the pressure membrane(s). If there is no correlation with DCM pressure, the pressure membrane might be ruptured. Throughout the roughing process (to ≈0.05 Torr) belljar and cell are pumped in parallel by P1/P2

   º Expected elapsed time: 2 hr to reach 1Torr

III. Transition

10. Open V6.
11. Start P3 (turbomolecular pump, aka turbine or turbo) at a pressure of 50 µ.
12. When P3 is up to speed (≈14 krpm, ≈30 min.) close V3 and V7. Belljar pressure should drop into the 10^{-5} Torr range.
13. If cell pressure remains high, He leak check and repair leaks.
14. Relocate RGA (residual gas analyzer) to belljar, evacuate plenum, He leak check, repair leaks.

    Notes: º If turbo controller frequency and power LED's do not light up when the START switch is pressed, check that pins 13 & 5 on J22 are shorted. If only the frequency LED's light up, check F2

    º From this point (11) belljar and cell are pumped separately. Monitoring DCM is no longer necessary except in the event of a problem. Before evaporation close the DCM manifold valves

IV. Glow Discharge Cleaning

15. Close V4, 5.
16. Admit glow gas targeting partial pressures of 5μ Ar, and 5μ O_2.
17. Adjust power supply for 650-700vac (see last note below). Glow for 30min.
18. Close O_2 metering valve, meter Ar to (target) 10μ.
19. Glow for an additional 15min.
20. Close Ar metering valve, Ar and O_2 shutoff valves, turn power off.

Notes:
- Glow discharge cleaning can commence at any time after cryopumps are fully operational. Generally, the more time the chamber spends at high vacuum the better
- Glow should be observed through the viewports
- Monitor color (Ar-violet, O_2-green) and maintain pressure between 10-20μ
- Terminate glow and investigate if any serious arcing is observed
- During the glow, the chamber is continuously pumped with P3 (cell is continuously backed with P1/P2)
- The desired power point is where the series elements (light bulbs) are regulating current—in this region changes in variac position will have little effect on the output voltage

V. Cryopumping

21. Verify P4, 5 temperatures/pressures.
22. Open V4, 5.

Notes:
- The outgassing rates of most materials reach a constant value after ≈4hr
- Cryopump LN_2 reservoirs should need filling about every 2-3hr
- Second stage temperatures should stabilize at ≤15K (typically 11)
- First stage temperatures should stabilize at ≤100K (typically 80)
- If the compressors shut themselves off, most likely there is a problem with coolant flow

VI. Evaporation

Necessary conditions:

- Cryopumps fully operational
- Pressure ≤8 x 10^{-6}Torr. It should be in the low 6's or better. (Acceptable films can be produced with starting pressures as high as $5x10^{-5.}$ This would indicate a problem, probably large leaks either from atmosphere or through the membrane, but properties of the resultant film are only marginally compromised)
- Center and edge thickness monitors ready
- RGA, data acquisition unit ready

Systems to be monitored by eye:

- Pressure
- Deposition rate
- Film thickness
- Time

23. Start data acquisition, RGA scan. Note time, pressure.
24. Ramp filament current up until all filaments are glowing a dull red. This will require ≈1000 amp/module. Some pressure rise will occur initially and should then drop off.
25. After perhaps 30 sec wetting will begin. This will be evidenced by a darkening of the wetting filaments resulting in a noticeable modulation of light intensity in the chamber. At this point rapidly ramp current to ≈1200 amp/module.
26. Regulate deposition rate with applied current. Target—100 Å/sec.
27. Target thickness—950 Å.

Notes:
- Terminate evaporation if the rate falls below 15 Å/sec
- Rate should be constant until shutoff. If it begins to fall off substantially toward the end DO NOT increase current in an attempt to maintain rate. Stop, investigate, reload and reshoot if necessary
- Pressure will initially rise into the low 5's (i.e. several times 10^{-5} Torr). It should then decrease to or below the starting pressure
- Max acceptable pressure at end of deposition—5 x 10^{-5} Torr
- Modules should remain out of fault and balanced ±5% throughout the evaporation. Terminate if more than 1 module goes out of balance or smokes

VII. Acceptance Criteria

We will accept the shoot if all of the following conditions are met:

- Thickness ≥750 Å
- Deposition rate at the end of evaporation ≥20 Å/sec
- Pressure at the end of evaporation ≤5x10^{-5} Torr
- Witness slides survive qualitative adhesion test (tape)
- Mean reflectance ≥88% @ 4500 Å

VIII. Logged Data

- Chamber total pressure vs. time
- Chamber partial pressure H_2 , N_2, O_2 vs. time
- Deposition rate vs. time
- Module power vs. time
- Film thickness

IX. Emergency Procedures

Catastrophic vent to atmosphere during roughing:

- Open V2 & 3
- Turn off blower (if on)
- Close V1

Catastrophic vent to atmosphere during transition:

- Open V2 & 3
- Turn off turbo controller
- Turn off blower
- Close V1

Catastrophic vent to atmosphere during high-vacuum pumping:

- Open V2 & 3
- Turn off turbo controller
- Turn off blower
- Close V1
- Close V4, 5
- Turn off He compressors

Notes:
- In all cases an emergency vent will rupture the membrane(s) and necessitate opening the belljar. If the membranes are compromised (leaking but not ruptured) the belljar ultimate pressure will determine go or no-go
- The turbopump's bearings might have to be inspected/replaced at the factory if vented to atmosphere while at full rpm
- The Roots blower should survive a vent as long as power is removed. If it is driven against an atmosphere it will overheat and likely self-destruct
- No issue with the mechanical or cryopumps venting

X. Shutdown

- Close V4, 5
- Turn off He compressors
- Turn off turbo controller. Turbine must spin down to 9 krpm or less before venting
- Close V6
- Close V1, turn off blower
- Open V2 & 3
- Simultaneously open V9 & 10

Appendix D. Power system schematic

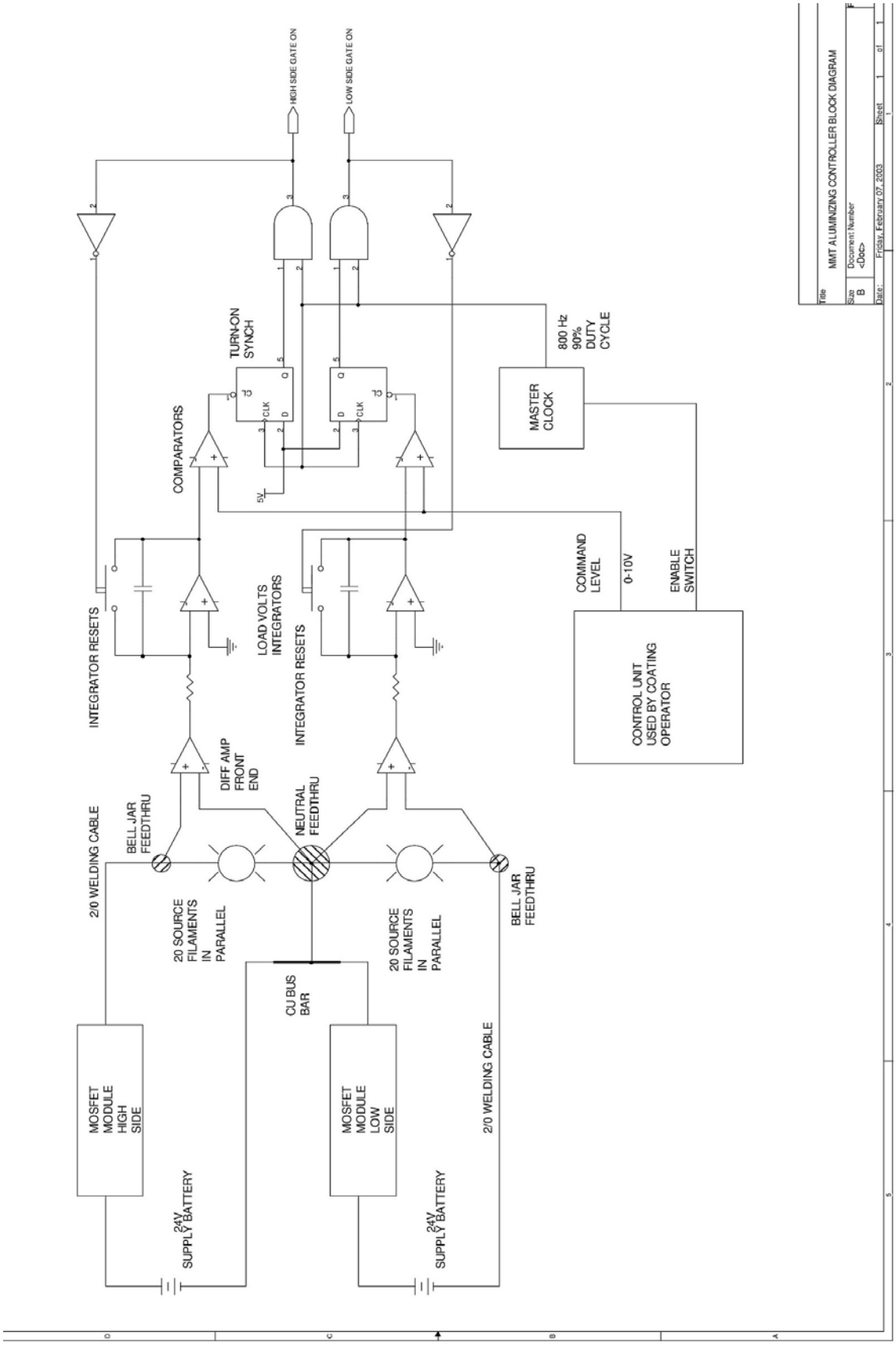

Further Reading

- J. Strong, "The Evaporation Process and its Application to the Aluminizing of Large Telescope Mirrors," Astrophys. J. **83**, 401-423 (1936).
- L. Holland and W. Steckelmacher, "The Distribution of Thin Films Condensed on Surfaces by the Vacuum Evaporation Method," Vacuum **2**, 346-364 (1952).
- S. Bateson, "Aluminum Reflecting Films Applied to Glass and Plastics by Thermal Evaporation," Vacuum **2**, 365-376 (1952).
- P. H. Berning, G. Haas, and R. P. Madden, "Reflectance-Increasing Coatings for the Vacuum Ultraviolet and Their Applications," J. Opt. Soc. Am. **50**, 586-597 (1959).
- K. H. Behrndt, "Film-Thickness and Deposition-Rate Monitoring Devices and Techniques for Producing Films of Uniform Thickness," in *Physics of Thin Films*, G. Haas and R. E. Thun, eds. (Academic, New York, 1966), Vol. 3, pp. 1-59.
- P. Bradford, G. Haas, J. F. Osantowski, and A. R. Toft, "Preparation of Mirror Coatings for the Vacuum Ultraviolet in a 2-m Evaporator," Appl. Opt. **8**, 1183-1189 (1969).
- L. V. Omelka, "Selective Pumping of an 800,000 ℓ Chamber," J. Vac. Sci. Technol. **7**, 257-261 (1970).
- E.T. Hutcheson, G. Hass, and J.T. Cox, "Effect of Deposition Rate and Substrate Temperature on the VUV Reflectance of MgF_2 and LiF-Overcoated Aluminum Mirrors," Appl. Opt. **11**, 2245-2248 (1972).
- W. Heitmann, "Reactively Evaporated Films of Scandia and Yttria," Appl. Opt. **12**, 394-397 (1973).
- J. A. F. Trueman, "The Design and Operation of Large Telescope Mirror Aluminizers," in *Proceedings of the 22nd Annual Technical Conference of the Society of Vacuum Coaters* (SVC, Washington, D.C., 1979), pp. 32-39.
- I. Lubezky, E. Ceren, and Z. Klien, "Silver Mirrors Protected with Yttria for the 0.5-14μm Region," Appl. Opt. **19**, 1895 (1980).
- S. F. Pellicori, "Scattering Defects in Silver Mirror Coatings," Appl. Opt. **19**, 3096-3098 (1980).
- F. M. Reicha and P. B. Barna, "Growth of Hillocks and Whiskers in Aluminium Films," Thin Solid Films **85**, 317 (1981).
- P. B. Barna, Z. Bodo, G. Gergely, P. Croce, J. Adam, and P. Jakab, "Ellipsometric and X-ray Specular Reflection Studies on Naturally Grown Overlayers on Aluminum Thin Films," Thin Solid Films **120**, 249-256 (1984).
- E. D. Erikson, T. G. Beat, D. D. Berger, and B. A. Frazier, "Vacuum Outgassing of Various Materials," J. Vac. Sci. Technol. A **2**, 206-210 (1984).
- R. Zito, W. S. Bickel, and W. M. Bailey, "The Physical and Optical Properties of Agglomerated Gold Films," Thin Solid Films **114**, 241-255 (1984).
- W. G. Sainty, R. P. Netterfield, and P. J. Martin, "Protective Dielectric Coatings Produced by Ion-Assisted Deposition," Appl. Opt. **23**, 1116-1119 (1984).
- D. Song, R. W. Sprague, H. A. Macleod, and M. R. Jacobsen, "Progress in the Development of a Durable Silver-Based High-Reflectance Coating for Astronomical Telescopes," Appl. Opt. **24**, 1164-1170 (1985).
- M. J. Verkerk and W. A. M. C. Brankae, "The Effects of Water on the Growth of Aluminum Films Deposited by Vacuum Evaporation," Thin Solid Films **139**, 77-88 (1986).
- J. R. Chen and Y. C. Liu, "A Comparison of Outgassing Rate of 304 Stainless Steel and A6063-EX Aluminum Alloy Vacuum Chamber after Filling with Water," J. Vac. Sci. Technol. A **5**, 262-264 (1987).
- J. I. Larruquert, J. A. Méndez, and J. A. Aznárez, "Far-UV Reflectance of UHV-prepared Al Films and its Degradation after Exposure to O_2," Appl. Opt. **33**, 3518-3522 (1994).
- D. Nahrstedt, T. Glesne, J. McNally, J. Kenemuth, and B. Magrath, "Electroless Silver as an Optical Coating in an Operational Environment," Appl. Opt. **35**, 3680-3686 (1996).
- S. S. Hayashi, Y. Kamata, T. Kanzawa, A. Miyashita, M. Nakagiri, T. Nishimura, T. Noguchi, K. Okita, N. Oshima, G. Sasaki, Y. Torii, M. Yutani, and T. Ishikawa, "Status of the Coating Facility of Subaru Telescope," in *Advanced Technology Optical/IR Telescopes VI*, L. M. Stepp ed., Proc. SPIE **3352** (1998), pp. 454-462.
- A. Guthrie, *Vacuum Technology* (Wiley, New York, 1963).
- R. P. LaPelle, *Practical Vacuum Systems* (McGraw-Hill, New York, 1972).
- L. Holland, W. Steckelmacher, and J. Yarwood, eds., *Vacuum Manual* (E. & F. N. Spon, London, 1974).
- R. V. Stuart, *Vacuum Technology, Thin Films and Sputtering* (Academic, New York, 1983).
- H. K. Pulker, *Coatings on Glass* (Elsevier, Amsterdam, 1984).
- H. A. McLeod, *Thin Film Optical Filters,* 2nd ed. (Macmillan, New York, 1986).

- N. Harris, *Modern Vacuum Practice* (McGraw-Hill, Berkshire, 1989).
- J. F. O'Hanlon*, A User's Guide to Vacuum Technology* (Wiley, New York, 1989).
- A. Chambers, R. K. Fitch, and B. S. Halliday, *Basic Vacuum Technology* (Hilger, Bristol, 1989).
- K. M. Welch, *Capture Pumping Technology: An Introduction* (Pergamon, New York, 1991).
- A. Berman, *Vacuum Engineering Calculations, Formulas, and Solved Exercises* (Academic, San Diego, 1992).
- H. Bach and D. Krause, eds., *Thin Films on Glass* (Springer, New York, 1997).

References

1. G. Haas and J. E. Waylonis, "Optical Constants and Reflectance and Transmittance of Evaporated Aluminum in the Visible and Ultraviolet," J. Opt. Soc. Am. **51**, 719-722 (1961).
2. G. Haas, "Filmed Surfaces for Reflecting Optics," J. Opt. Soc. Am. **45**, 945-952 (1955).
3. E. T. Hutcheson, G. Haas, and J. K. Coulter, "A Direct Comparison of the Visible and Ultraviolet Reflectance of Aluminum Films Evaporated in Conventional and Ultra-High Vacuum Systems," Opt. Commun. **3**, 213-216 (1971).
4. H. E. Bennett, J. M. Bennett, and E. J. Ashley, "Infrared Reflectance of Evaporated Aluminum Films," J. Opt. Soc. Am. **52**, 1245-1250 (1962).
5. H. E. Bennett, M. Silver, and E. J. Ashley, "Infrared Reflectance of Aluminum Evaporated in Ultra-High Vacuum," J. Opt. Soc. Am. **53**, 1089-1095 (1963).
6. G. Haas and L. Hadley, "American Institute of Physics Handbook," 3rd ed., D. E. Gray, ed. (McGraw-Hill, New York, 1972), pp. 6-124,125,157.
7. G. Haas, J. B. Heaney, and W. R. Hunter, "Reflectance and Preparation of Front Surface Mirrors for Use at Various Angles of Incidence from the Ultraviolet to the Far Infrared," in *Physics of Thin Films*, G. Haas, M. H. Francombe, and J. L. Vossen, eds. (Academic, New York, 1982), Vol. 12, pp. 1-51.
8. J. M. Hill, "Optical Design, Error Budget and Specifications for the Columbus Project Telescope," in *Advanced Technology Optical Telescopes IV,* L. D. Barr ed., Proc. SPIE **1236** (1990), pp. 86-107. http://medusa.as.arizona.edu/lbtwww/tech/spieopti.htm.
9. J. M. Hill, "Error Budget and Wavefront Specifications for Primary and Secondary Mirrors," LBT Project Technical Memorandum **UA-94-01** (1994), http://medusa.as.arizona.edu/lbtwww/tech/ua9401.htm.
10. D. Fabricant, B. McLeod, and S. West, "Optical Specifications for the MMT Conversion," MMT Technical Report **35** (1999).
11. W. B. Davison and J. T. Williams, "Basic Considerations for the Design of a Vacuum Aluminizing Chamber for the Columbus Project," Columbus Project Technical Memorandum **UA-87-21** (1987).
12. W. B. Davison, "Aluminizing the Mirrors in the Telescope," Columbus Project Technical Memorandum **UA-88-01** (1988).
13. W. B. Davison, "Definition of the Aluminizing Chamber for Cost Estimates," Columbus Project Technical Memorandum **UA-88-15** (1988).
14. G. Haas and C. D. Salsberg, "Optical Properties of Silicon Monoxide in the Wavelength Region from 0.24 to 14.0 Microns," J. Opt. Soc. Am. **44**, 181-187 (1954).
15. A. P. Bradford and G. Haas, "Increasing the Far-Ultraviolet Reflectance of Silicon-Oxide-Protected Aluminum Mirrors by Ultraviolet Radiation," J. Opt. Soc. Am. **53**, 1096-1100 (1963).
16. H. E. Bennett, J. M. Bennett, and E. J. Ashley, "The Effect of Protective Coatings of MgF_2 and SiO on the Reflectance of Aluminized Mirrors," Appl. Opt. **2**, 156 (1963).
17. J. T. Cox, G. Haas, and W. R. Hunter, "Infrared Reflectance of Silicon Oxide and Magnesium Fluoride Protected Aluminum Mirrors at Various Angles of Incidence from 8μm to 12μm," Appl. Opt. **14**, 1247-1250 (1975).
18. G. Haas, J. B. Heaney, H. Herzig, J. F. Osantowski, and J. J. Triolo, "Reflectance and Durability of Ag Mirrors Coated with Thin Layers of Al_2O_3 plus Reactively Deposited Silicon Oxide," Appl. Opt. **14**, 2639-2644 (1975).
19. J. T Cox and G. Haas, "Aluminum Mirrors Al_2O_3 Protected, with High Reflectance at Normal but Greatly Decreased Reflectance at Higher Angles of Incidence in the 8-12μm Region," Appl. Opt. **17**, 333-334 (1978).
20. J. T Cox and G. Haas, "Protected Al Mirrors with High Reflectance in the 8-12μm Region from Normal to High Angles of Incidence," Appl. Opt. **17**, 2125-2126 (1978).

21. W. A. Pliskin, D. R. Kerr, and J. A. Perri, "Thin Glass Films," in *Physics of Thin Films*, G. Haas, ed. (Academic, New York, 1967), Vol. 4, pp. 247-324.

22. E. Ritter, "Dielectric Film Materials for Optical Applications," in *Physics of Thin Films*, G. Haas and M. H. Francombe, eds. (Academic, New York, 1975), Vol. 8, pp. 1-49.

23. R. P. Madden, L. R. Canfield, and G. Haas, "On the Vacuum-Ultraviolet Reflectance of Evaporated Aluminum Before and During Oxidation," J. Opt. Soc. Am. **53**, 620-625 (1963).

24. R. W. Springer and D. S. Catlett, "Rate and Pressure Dependence of Contaminants in Vacuum-Deposited Aluminum Films," J. Vac. Sci. Technol. **15**, 210-214 (1977).

25. L. F. Drummeter, Jr. and G. Haas, "Solar Absorptance and Thermal Emittance of Evaporated Coatings," in *Physics of Thin Films*, G. Haas and R. E. Thun, eds. (Academic, New York, 1964), Vol. 2, pp. 305-361.

26. L. Holland, *Vacuum Deposition of Thin Films* (Wiley, New York, 1956), pp. 123-124.

27. D. M. Mattox, "Atomistic Film Growth & Resulting Film Properties—Pinholes," Vac. Technol. Coat. **2**, 32-34 (2001).

28. J. M. Hill and M. P. Lesser, "Notes on Aluminizing 8-meter Mirrors," Columbus Project Technical Memorandum **UA-88-06** (1988).

29. B. A. Sabol, B. Atwood, J. M. Hill, J. T. Williams, M. P. Lesser, P. L. Byard, and W. B. Davidson, "Evaporative Coating Systems for Very Large Astronomical Mirrors," in *Advanced Technology Optical Telescopes 1V,* L. D. Barr ed., Proc. SPIE **1236** (1990), pp. 940-951, http://medusa.as.arizona.edu/lbtwww/tech/evapor.htm.

30. B. A. Sabol, J. M. Hill, B. Atwood, P. L. Byard, T. P. O'Brien, and J. A. Mason, "Aluminization Research for the Large Binocular Telescope," LBT Project Technical Memorandum **UA-93-05** (1993).

31. L. Holland, "The Effect of Vapor Incidence on the Structure of Evaporated Aluminum Films," J. Opt. Soc. Am. **43**, 376-380 (1953).

32. A. Mazor, B. G. Bukiet, and D. J. Srolovitz, "The Effect of Vapor Incidence Angle on Thin-film Columnar Growth," J. Vac. Sci. Technol. A **7**, 1386-1391 (1989).

33. F. Abelès, "Optical Properties of Metallic Films," in *Physics of Thin Films*, M. H. Francombe and R. W. Hoffman, eds. (Academic, New York, 1971), Vol. 6, pp. 151-205.

34. J. I. Larruquert, J. A. Méndez, and J. A. Aznárez, "Empirical Relations Among Scattering, Roughness Parameters, and Thickness of Aluminium Films," Appl. Opt. **32**, 6341- 6346 (1993).

35. D. M. Mattox, *Handbook of Physical Vapor Deposition (PVD) Processing* (Noyes, Park Ridge, NJ, 1998), pp. 482-486.

36. L. Holland [26] op. cit., pp. 74-94.

37. B. A. Sabol, "Glow Discharge Cleaning—Review and Recommendations," MMT Conversion Technical Memorandum **89-1** (1989).

38. J. Strong, "On the Cleaning of Surfaces," Rev. Sci. Instrum. **6**, 97-98 (1935).

39. G. V. Jorgenson and G. K. Wehner, "Pinholes in Thin Films," in *Transcripts of the 10th National Vacuum Symposium* (Macmillan, New York, 1963), pp. 388-392.

40. K. H. Guenther, L. Penney, and R. R. Willey, "Corrosion-Resistant Front Surface Aluminum Mirror Coatings," Opt. Eng. **32**, 547-552 (1993).

41. J. R. Varsik, W. A. Siegmund, and D. H. Berger, "Telescope Mirror Contamination and Airborne Dust," presented at AAS Solar Physics Division Annual Meeting, Bozeman, MT, 27 June – 1 July, 1997.

42. P. Giordano, "Paranal Dust Survey: Part 2—Evaluation of Cleaning Techniques on Mirrors Exposed in the Open Air at Paranal," ESO VLT Technical Report **11942-1305** (1997).

43. S. A. Hoenig, "Cleaning Surfaces with Dry Ice," Compressed Air **91**, 22-25 (1986).

44. S. A. Hoenig, Dept. of Electrical and Computer Engineering, University of Arizona, unpublished DOD manuscript "The Application of Dry Ice and Ultraviolet Light to the Removal of Particulates from Optical Apparatus, Spacecraft, Semiconductor Wafers and Equipment Used in Contaminant Free Manufacturing Processes," (1987).

45. W. H. Whitlock, "Dry Surface Cleaning with CO_2 Snow," Presented at Fine Particle Society 20th Annual Meeting, Boston, MA, 22 August, 1989.

46. R. R. Zito, "Cleaning Large Optics with CO_2 Snow," in *Advanced Technology Optical Telescopes 1V,* L. D. Barr ed., Proc. SPIE **1236** (1990), pp. 952-971.

47. W. D. Kimura and G. H. Kim, "Comparison of Laser and CO_2 Snow for Cleaning Large Astronomical Mirrors," Publ. Astron. Soc. Pac. **107**, 888-895 (1995), http://www.gemini.edu/documentation/webdocs/rpt/rpt-te-g0074.pdf

48. B. Magrath, “Reflectivity Degradation Rates of Aluminum Coatings at the CFHT,” Publ. Astron. Soc. Pac. **109**, 303-306 (1997).

49. Y. Naeba, H. Yoshikawa, H. Yanagida, H. Yamakawa, and S. Komiya, “A He-Ne Laser-SEM Combined Monitor for In Situ Observation of Dust Laid on a Substrate in Vacuum,” Presented at Electrochemical Society Conference, Toronto, Canada, 16 May, 1985.

50. J. A. Schier, “Mirror Thermal Behavior During Aluminization,” Magellan Project Internal Memorandum to W. A. Hiltner, March 9, 1989.

51. John Lombardo, Chart Inc.-Process Systems Division (formerly HVEC), 115 Flanders Rd., Suite 200, Westborough, MA 01581, personal communication, 1995).

52. N. A. Walter and J. A. Scialdone, “Outgassing Data for Selecting Spacecraft Materials,” NASA Reference Publication **1124**, Rev. 4 (1997), http://outgassing.nasa.gov/.

53. M. H. Hablanian, *High Vacuum Technology* (Dekker, New York, 1990), pp. 240.

54. G. J. van der Kolk and M. J. Verkerk, “Microstructural Studies of the Growth of Aluminum Films with Water Contamination,” J. Appl. Physics **59**, 4062-4067 (1986).

55. A. P. M. Glassford and C. K. Liu, “Outgassing Rate of Multilayer Insulation Materials at Ambient Temperature,” J. Vac. Sci. Technol. **17**, 696-704 (1980).

56. B. A. Sabol, “Mirror Coating at the Sunnyside Facility—An Operational Guide,” MMT Internal Technical Memorandum **88-3** (1988), pp. 3-5.